communications biology

A Nature Portfolio journal

Article

https://doi.org/10.1038/s42003-025-08223-4

A type III-associated Cas6 functions as a negative regulator of type I-B CRISPR-Cas system in *Thermus thermophilus*

Junwei Wei[1], Yuan Shao[1], Yuqian Liang[1], Xuying Bu[1], Wen Zhou[2], Yunxiang Liang[1] & Yingjun Li[1]

CRISPR-Cas systems are small RNA-guided immune systems in prokaryotes. CRISPR RNA (crRNA) provides sequence specificity and programmability, guiding the effector complex to cleave target nucleic acids. Cas6 family ribonucleases can cleave precursor crRNA to generate functional crRNAs in most type I and type III CRISPR-Cas systems. Most existing studies of Cas6 functions are mainly focused on nuclease activity in vitro and Cas6-processed product characterization in vivo. However, in hosts harboring multiple CRISPR systems, the biological functions of the co-occurrence of various Cas6 proteins and their cross-cleavage activity toward different types of crRNAs remain largely unexplored. In this study, we biochemically characterized the cross-cleavage activity of two Cas6 proteins in *Thermus thermophilus* HB27 and first found that Cas6 could anchor the mature crRNA and interact with Cas5 subunit of type I-B system, revealing the functions of Cas6 to mediate the assembly of type I Cascade complex. We further demonstrated that the type III-associated Cas6 protein could act as a negative regulator by competing with the I-B Cas6 protein during the assembly of type I-B Cascade complex, significantly suppressing the interference activity of type I-B system. Our findings provide an insight into the functional coupling and regulation mechanisms underlying multiple CRISPR-Cas systems.

The clustered regularly interspaced short palindromic repeats (CRISPR) and CRISPR-associated (Cas) protein (CRISPR-Cas) system is an extensively distributed adaptive and heritable immune system in prokaryotes, endowing them with the ability to resist invasions by foreign mobile genetic elements such as bacteriophages[1–3]. An active CRISPR-Cas system is composed of *cas* gene operons and CRISPR arrays that consist of a set of conserved short direct repeats separated by unique spacers[4]. These spacers originated from exogenous mobile genetic elements form an immune memory[1]. CRISPR-Cas system is currently classified into two classes (Class 1 and Class 2), including six main types (Types I-VI), which are further subdivided into more than 30 distinct subtypes[5–7]. All types of CRISPR-Cas systems share a three-step immunity process: Step 1 Spacer acquisition, where invading nucleic acid fragments are integrated into the CRISPR array by the adaptation complex composed mainly of Cas1 and Cas2, thus forming new spacers; Step 2 CRISPR RNA (crRNA) biogenesis, where the precursor crRNA (pre-crRNA) is transcribed from the CRISPR array and processed by Cas proteins or intracellular ribonucleases into small mature crRNAs; and Step 3 Interference, where the mature crRNAs assemble with one or more Cas proteins into an effector complex (Cascade, CRISPR-associated complex for antiviral defense) that specifically cleaves the invading nucleic acids[8].

Both type I and type III CRISPR-Cas systems can employ multi-subunit effector complexes to defend against invading nucleic acids, and they have a close phylogenetic relationship, and their effector complexes exhibit a high similarity in the composition[9]. crRNA is necessary for the function of CRISPR-Cas systems, guiding the CRISPR effector complex to cleave the target nucleic. It confers unique sequence specificity and programmability to CRISPR-Cas systems, which is the key feature that distinguishes CRISPR-Cas systems from other endonucleases. Generally, repeat sequences of most type I and type III CRISPR-Cas systems can form stable hairpin structures, which is crucial for repeat sequence recognition by Cas6 (except recognition by Cas5 in subtype I-C system)[10–14]. Cas6-mediated cleavage produces mature crRNAs bearing a unique spacer sequence flanked by an 8-nucleotide 5' handle and a 3' stem loop derived from the repeat sequence[15,16]. In most CRISPR-Cas systems, Cas6 proteins form monomers, while they form dimers in only a few systems, mainly

[1]National Key Laboratory of Agricultural Microbiology, College of Life Science and Technology, Huazhong Agricultural University, Wuhan, PR China. [2]Green Chemical Reaction Engineering, Engineering and Technology Institute Groningen (ENTEG), University of Groningen, Groningen, AG, The Netherlands.
e-mail: yingjun@mail.hzau.edu.cn

including I-A and I-B, and the dimeric organization is essential for their cleavage activity[15,17,18]. Type I and type III systems often co-occur and share crRNA-processing proteins and even CRISPR arrays[9,19–21], suggesting their potential cooperation and unique functionality[22,23]. The cross-cleavage activity of Cas6 on different types of crRNAs has been reported in hosts harboring multiple CRISPR-Cas systems, specifically in *Sulfolobus solfataricus*[24], *Methanosarcina mazei*[25], and *Anabaena* sp.[26]. Most Cas6 proteins of type I systems remain anchored to the processed crRNA to assist in the assembly of the Cascade complex[27–29]. The backbone of both type I and type III complexes is composed of repeat-associated mysterious proteins (RAMPs) such as Cas7 and Cas5, as well as "large" and "small" subunits[30–33]. Typically, in type III CRISPR-Cas systems, a further trimming of the downstream 3' stem loop of Cas6-processed crRNA is required to generate the active mature crRNA[34]. Accordingly, most type III interference effector complexes contain no Cas6 protein[35,36].

Hyperthermophilic Gram-negative bacterium *Thermus thermophilus* usually encodes multiple CRISPR-Cas systems located on the chromosome and/or on megaplasmid[37]. *Thermus thermophilus* is frequently used for investigating the mechanisms of CRISPR-Cas systems[38–41]. RNA sequencing demonstrates that there are mainly two pre-crRNA processing mechanisms operating simultaneously in *T. thermophilus* HB8[42]. The structure analysis of two Cas6-crRNA complexes in *T. thermophilus* HB8 has indicated that two types of repeat sequences are subjected to cross-cleavage by Cas6, and that both 3' stem-loop and the 5'-segment of the repeat sequence are indispensable for crRNA recognition by Cas6[43]. Currently, most studies of Cas6 in type I and III systems are mainly focused on in vitro nuclease activity of Cas6 and in vivo processed product characterization. However, the phenomena of co-occurrence and cross-cleavage of different Cas6 proteins in a multi-CRISPR system host remains largely unexplored.

In this study, we identified the proteins responsible for processing crRNA in four types of CRISPR-Cas systems in *T. thermophilus* HB27 and found the differences in interference activity among these systems. We biochemically characterized the cross-cleavage activity of two Cas6 proteins towards different types of crRNAs, revealed the functions of Cas6 to anchor the mature crRNA and interact with Cas5 subunit of type I-B systems for the first time, and elucidated a clear pattern of type I-B Cascade complex assembly. We further demonstrated that the type III-associated Cas6 protein could act as a negative regulator by competing with the I-B Cas6 protein during the assembly of type I-B Cascade complex, thereby significantly suppressing the interference activity of type I-B system. Overall, this study provides insight into the functional coupling and regulation among multiple CRISPR-Cas systems.

Results

Specificity of CRISPR arrays among endogenous CRISPR-Cas systems in *T. thermophilus* HB27

The genome of *T. thermophilus* HB27 strain maintained in our laboratory encodes 4 subtypes of CRISPR-Cas systems (I-B, I-C, III-A, and III-B) and 11 CRISPR arrays composed of three different types of repeat sequences (Fig. 1a and Table 1)[38]. Repeat-1 and Repeat-3 exhibit high similarity in sequence and structure, whereas Repeat-2 is significantly different from the other two (Fig. 1b). CRISPR-Cas immunity protects cells from invading mobile genetic elements such as bacteriophages and plasmids. Therefore, plasmid interference assays were performed to assess the in vivo defense activity of CRISPR systems in this study. Figure 1c illustrates three plasmid interference strategies: Strategies 1 and 2 employ an interference plasmid carrying an artificial mini-CRISPR array to generate crRNAs that direct the endogenous CRISPR-Cas system to target the host genome or the plasmid itself; Strategy 3 introduces an invader plasmid containing target sequences complementary to genomic CRISPR spacers, enabling CRISPR-Cas-mediated clearance. Therefore, functional CRISPR-Cas systems are predicted to markedly reduce both host viability and transformation efficiency of exogenous plasmids (Fig. 1c).

To determine whether the CRISPR arrays of *T. thermophilus* HB27 exhibit specificity among different subtypes of CRISPR-Cas systems, we constructed a series of deletion mutants (denoted by ΔI-B, ΔI-C, ΔIII-A, and ΔIII-B) of CRISPR-Cas systems in HB27, iterative deletion mutants (ΔIII-AB and ΔIII-ABΔI-C) of multiple subtype systems, and a deletion mutant (ΔCRISPR) of all CRISPR-Cas systems (Supplementary Fig. 1). Subsequently, plasmid interference in these deletion mutants in vivo was analyzed by strategy 1 mentioned above. Three artificial mini-CRISPR plasmid vectors containing Repeat-1 (denoted by pRKP31-AC1), Repeat-2 (pRKP31-AC2), and Repeat-3 (pRKP31-AC3) were constructed (Supplementary Table 1). Subsequently, two spacers that could target an essential gene encoding the α subunit of DNA polymerase III (*DNApolyα*) in HB27 were cloned into multiple vectors of pRKP31-AC to obtain interference plasmids. In detail, III-A/B spacer (a spacer of type III-A and III-B systems, exhibiting the interference characteristics due to the mismatch between the 5'-handle sequence of the crRNA and the 3' flanking sequence of the protospacer) was cloned into the pRKP31-AC1 to obtain pAC1-DNApolyα-III. Accordingly, I-B/I-C spacer targeting the protospacer with TTC PAM motif (an active PAM for the type I-B and type I-C systems in HB27[38]) was cloned into pRKP31-AC2 and pRKP31-AC3 separately to obtain pAC2-DNApolyα-I and pAC3-DNApolyα-I. As shown in Fig. 1d, artificial mini-CRISPR plasmids without spacer exhibited a high strain transformation efficiency (about 1×10^4 CFU/μg plasmid DNA), while the Repeat-1-derived plasmid pAC1-DNApolyα-III hardly displayed transformation efficiency to the strains carrying type III-A or type III-B system, suggesting that Repeat-1 conferred both type III-A and type III-B systems with strong defense activity (Fig. 1d). The Repeat-2-derived plasmid pAC2-DNApolyα-I showed a high transformation efficiency only to 3 type I-C deletion mutants (ΔI-C, ΔIII-ABΔI-C, and ΔCRISPR), indicating a lack of interference activity of these mutant strains (Fig. 1e). The deletion of type I-B systems (ΔI-B and ΔCRISPR) resulted in a ~10^3-fold increase in the transformation efficiency of Repeat-3-derived plasmid pAC3-DNA polyα-I (Fig. 1f). Moreover, we examined the remaining combinations of three repeats and two spacers to further explore the possibility of cross-utilization of CRISPR arrays by different CRISPR-Cas systems. The results showed that even in the wild-type strain with all types of CRISPR-Cas systems intact, other mini-CRISPR combinations exhibited no interference activity (Supplementary Fig. 2). These findings indicated that the CRISPR arrays in HB27 had strong specificity among different CRISPR-Cas systems, and the arrays containing Repeat-1, Repeat-2, and Repeat-3 had specificity to the type III, type I-C, and type I-B systems, respectively.

Type III CRISPR-Cas systems exhibit stronger defense activity against multi-copy targets than type I systems in *T. thermophilus* HB27

To explore the differences in the defense activity against invading genetic elements among different endogenous subtypes of CRISPR-Cas system, we assessed the interference intensity of different CRISPR-Cas systems using three plasmid interference strategies described above (Fig. 1c). Specifically, strategy 1 used an interference plasmid to target *gyrA* gene located on chromosome or *hoxN* gene on megaplasmid; strategy 2 employed an interference plasmid to target the *puc* replicon on exogenous plasmid, and strategy 3 utilized three invader plasmids with each carrying a target sequence of spacer 1 in CRISPR arrays 2 (C2S1), 4 (C4S1), and 6 (C6S1) to detect the interference activity of III-AB, I-C and I-B CRISPR-Cas systems, respectively.

As shown in Fig. 1g, type III CRISPR-Cas system exhibited a high level of defense activity against its target sequence (either on the HB27 genome or on exogenous plasmid), with almost no transformants observed. Both type I-B and I-C exhibited strong interference activity against target sequence on the HB27 genome, whereas target sequence on exogenous plasmid appeared to evade the CRISPR immunity (Fig. 1g and Supplementary Fig. 3). Sequence analysis of escape transformants from the I-B and I-C systems revealed no sequence mutations in the CRISPR arrays or protospacer sites (Supplementary Fig. 4), indicating that the escape of transformants was due to the low interference activity of the I-B and I-C systems. The consistent results were also observed when using different targets, namely, type I

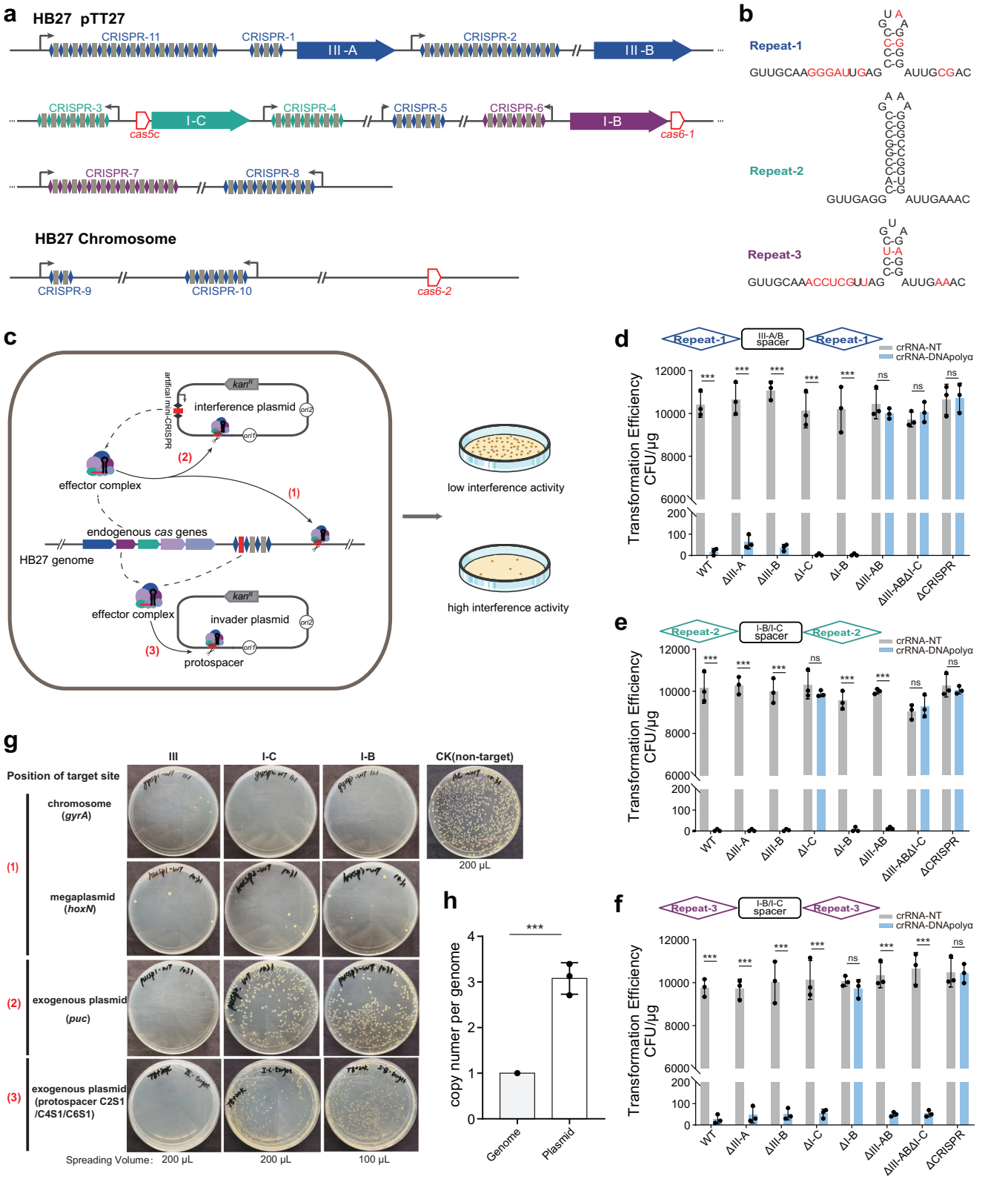

system of HB27 exhibited a significantly lower interference activity against exogenous plasmids than type III system (Supplementary Fig. 5). We speculated that the low interference activity of type I system might be due to the differences in copy numbers between the exogenous plasmid and the HB27 genome even though HB27 was a polyploid strain[44]. The copy numbers of the endogenous megaplasmid pTT27 and the chromosome have been reported to be identical[44]. Therefore, we further compared the copy numbers of exogenous plasmid and HB27 genome using quantitative real-time PCR (qPCR), and found that the copy number of the exogenous plasmid was approximately two times higher than that of the HB27 genome (Fig. 1h). The above results demonstrated significant differences in the abilities between the endogenous type I and type III CRISPR-Cas systems in

Fig. 1 | The specificity of CRISPR arrays among different CRISPR-Cas systems and the differences in defense activity of different CRISPR-Cas systems. **a** CRISPR-Cas loci distributed on HB27 megaplasmid pTT27 and chromosome. CRISPR arrays are numbered and categorized into 3 different types based on their Repeat variants, indicated by different colors. And the direction of their transcription is marked with arrows. **b** Sequences and predicated secondary structures of 3 different types of HB27 CRISPR repeats. Repeat-1 and Repeat-3 exhibit similarities in structure and sequence, with the differing bases between them highlighted in red. **c** Schematic diagram for the assessment of the interference activity of endogenous CRISPR-Cas systems through the transformation of exogenous plasmids. (1), (2) and (3) represent three plasmid interference strategies respectively: (1) and (2) use an interference plasmid which carry an artificial mini-CRISPR array to produce crRNAs to target the genome or the plasmid itself, (3) involves an invader plasmid carrying a protospacer designed based on the spacer sequence in endogenous CRISPR arrays. **d**, **e**, **f** Interference plasmids (crRNA-DNApolyα) built on three repeats and different spacers targeting the *DNApolyα* gene of *T. thermophilus* HB27 were used to detect the interference activity in a series of CRISPR-Cas system deletion strains and wild-type strain (WT). The combination diagram of repeats and spacers is shown in rectangles and diamonds of different colors. Non-target plasmid (crRNA-DNApolyα-NT) was used as control. **g** Results of plasmid transformation of *T. thermophilus* HB27 with self-targeting mini-CRISPR plasmids or invader plasmids containing protospacers for different endogenous CRISPR-Cas systems. *gyrA*, *hoxN*, and *puc* represent the three target genes located on chromosome, megaplasmid, and exogenous plasmid, respectively. Spacers in the mini-CRISPR plasmid were designed based on the sequences of these three genes. Protospacer C2S1/C4S1/C6S1 represents the invader plasmids carrying a target sequence of spacer 1 in CRISPR arrays 2, 4, and 6, which were used to detect the interference activity of III-AB, I-C, and I-B CRISPR-Cas systems, respectively. Non-target plasmid was used as control. To better calculate the number of colonies, the volume of bacterial suspension spread on the plates for the I-B group is only half of that for the I-C group. **h** The comparison of the copy number of *T. thermophilus* HB27 genome with the exogenous plasmid through quantitative PCR. The copy number of HB27 genome was normalized to 1, and the relative copy number of plasmid was determined accordingly. The data show means of three biological replicates. Error bars indicate the standard deviations (SD). Between-group significance was determined using the unpaired two-sample *t*-test (*$P < 0.05$, **$P < 0.01$, and ***$P < 0.001$). And ns indicates no significance.

Table 1 | CRISPR arrays characteristics of *T. thermophilus* HB27

CRISPR array	Repeat sequence	Repeat type	Repeat length (bp)	Spacer length (bp)
1, 2, 5, 8, 9, 10, 11	**GTTGCAAGGGATTGAGCCCCGTAAGGGGATTGCGAC**	1	36	34–47
3, 4	**GTTGCACCGGCCCGAAAGGGCCGGTGAGGATTGAAAC**	2	37	33–42
6, 7	**GTTGCAAACCTCGTTAGCCTCGTAGAGGATTGAAAC**	3	36	34–38

HB27 to defend against multi-copy targets. The strong interference activity of type III CRISPR-Cas system on invader plasmids might be attributed to the non-specific RNA cleavage by cOA-activated Csm6/Csx1 ribonucleases.

Determination of crRNA-processing endoribonucleases in CRISPR-Cas systems in *T. thermophilus* HB27

Two *cas6* genes (*cas6-1* at type I-B locus and *cas6-2* on the chromosome far away from any CRISPR locus) and one *cas5c* gene (at type I-C locus) have been identified in the *T. thermophilus* HB27 genome (Fig. 1a). In this study, we firstly created a series of gene deletion mutants for these 3 potential crRNA-processing endoribonuclease genes (Δ*cas6-1*, Δ*cas6-2*, and Δ*cas5c*) and their iterative deletion mutants (Δ*cas6-1,2 and* Δ*cas6-1,2,5c*) (Supplementary Fig. 6a). Subsequently, interference plasmids carrying spacers targeting the *DNApolyα* gene and the control plasmids were employed to investigate the interference activity in vivo of type III-A/B, I-C and I-B CRISPR-Cas systems respectively. The results showed that *cas6-2* absence from strain eliminated the interference activity of type III system (Fig. 2a); *cas5c* absence abolished the interference activity of type I-C system (Fig. 2b), and *cas6-1* absence deprived the interference activity of type I-B system (Fig. 2c), indicating that these 3 endoribonucleases, Cas6-2, Cas5c, and Cas6-1, might be responsible for the crRNA maturation in type III-A/B, I-C, and I-B CRISPR-Cas systems, respectively. We assessed the in vivo processing of precursor crRNA (pre-crRNA) by these endoribonucleases by RT-qPCR. The primers for RT-qPCR were designed between the leader sequence and the first spacer of each CRISPR array (Supplementary Table 2) to relatively quantify pre-crRNA unprocessed by endoribonucleases. Consistent with the interference plasmid assay results, the knock-out of *cas6-1*, *cas5c*, and *cas6-2* led to a significant increase in the accumulation of pre-crRNA from the respective CRISPR arrays (Supplementary Fig. 7). Notably, when *cas6-2* was absent, the levels of pre-crRNAs from CRISPR-6 and CRISPR-7 also increased significantly, suggesting cross-processing of pre-crRNAs by Cas6-2 in type I-B system (Supplementary Fig. 7).

To further explore the specificity in crRNA maturation, Cas6-1, Cas5c, and Cas6-2 proteins were expressed in *E. coli* and affinity purified (Supplementary Fig. 6b), and a series of in vitro cleavage assays were conducted to test their enzymatic properties. The cleavage assay on 5'-FAM-labeled repeats showed that substrate residues of Repeat-1 and Repeat-3, especially Repeat-3, were virtually undetectable within 10 s, and that two Cas6 proteins (Cas6-1 and Cas6-2) exhibited no cleavage activity on Repeat-2 in vitro, indicating that both Cas6-1 and Cas6-2 could efficiently cleave Repeat-1 and Repeat-3 in vitro (Fig. 2d, e). In contrast, Cas5c had strong cleavage activity on Repeat-2, whereas it exhibited very weak cleavage activity on Repeat-1 and Repeat-3 (Fig. 2f). Further, we examined the cleavage specificity of Cas6-1 and Cas6-2 using pre-crRNA substrates obtained from transcription in vitro and obtained similar results (Supplementary Fig. 8). Taken together, the above results collectively indicated that Cas5c might be exclusively responsible for crRNA processing of type I-C system, whereas Cas6-1 and Cas6-2 both might be in charge of crRNA processing of type III and type I-B systems.

Cas6-2 inhibits plasmid interference activity of type I-B CRISPR-Cas system in vivo

Considering cross-processing of type I-B pre-crRNA in vivo (Supplementary Fig. 7) and in vitro (Fig. 2e) by Cas6-2, we further investigated whether this cross-processing could interfere with the immunity activity of type I-B systems. Three invader plasmids carrying protospacer C2S1, C4S1, or C6S1 were used to detect the interference activity of type III-AB, I-C, and I-B CRISPR-Cas systems, respectively. Non-target plasmid was used as control. The results showed that the deletion of Cas6-2 and Cas5c abolished the interference activity of type III and I-C CRISPR-Cas systems, respectively (Fig. 3a, b). The plasmid interference activity of type I-B system was weak in wild-type strain, which was consistent with the above findings. And deletion of Cas6-1 further reduced the interference activity against invader plasmid, to a level that is no longer significantly different from the non-target control plasmid (Fig. 3c). Interestingly, the deletion of Cas6-2 led to a significant enhancement of the interference activity of type I-B system, enabling the complete elimination of the invader plasmid (Fig. 3c). Consistently, three another invader plasmids carrying protospacers C6S2, C7S1, and C7S2 were subjected to strong interference by type I-B system in Δ*cas6-2* strain

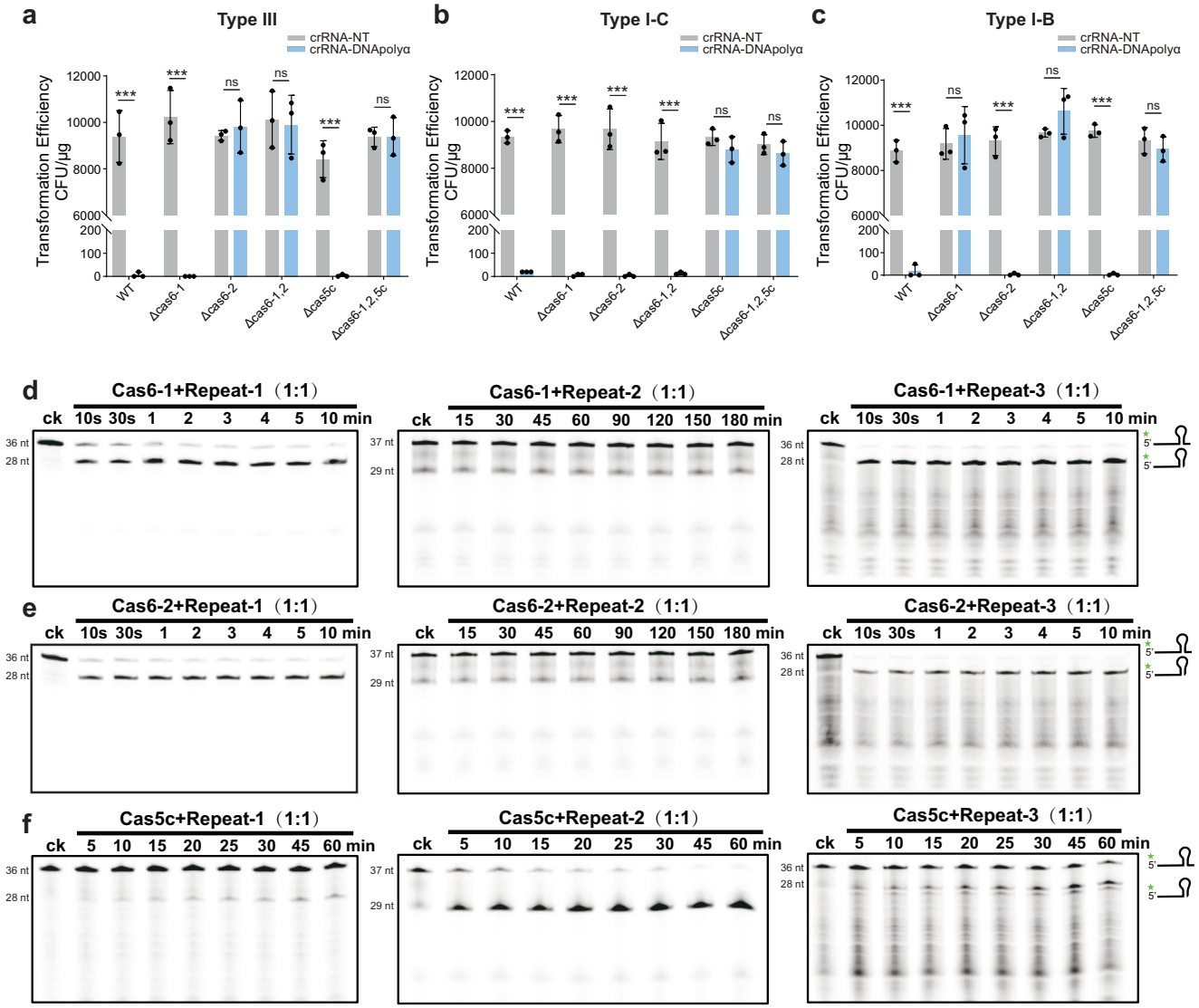

Fig. 2 | Determination of the crRNA processing proteins in *T. thermophilus* HB27. **a**, **b**, **c** The interference activity assay using interference plasmids for different endogenous CRISPR-Cas systems in various *T. thermophilus* HB27 strains. The interference plasmids carry mini-CRISPR arrays corresponding to different CRISPR-Cas systems, which are designed to target the *DNApolyα* gene on the *T. thermophilus* HB27 chromosome (crRNA-DNApolyα). Non-target plasmid was used as control (crRNA-NT). **d** The cleavage of 5' FAM-labeled Repeat-1, Repeat-2, and Repeat-3 by Cas6-1 over different time periods. **e** The cleavage of 5' FAM-labeled Repeat-1, Repeat-2, and Repeat-3 by Cas6-2 over different time periods. **f** The cleavage of 5' FAM-labeled Repeat-1, Repeat-2, and Repeat-3 by Cas5c over different time periods. The ck group indicates that no protein was added to the reaction system. The data show means of three biological replicates. Error bars indicate the standard deviations (SD). Between-group significance was determined using the unpaired two-sample *t*-test (*$P < 0.05$, **$P < 0.01$, and ***$P < 0.001$). And ns indicates no significance.

(Supplementary Fig. 9). Overall, these results demonstrated that type III associated Cas6-2 protein could suppress plasmid interference activity of type I-B system in *T. thermophilus* HB27.

Further, we cloned Cas6-1- and Cas6-2-encoding genes onto the interference plasmids to achieve supplementation or complementation (for deletion mutants) and examined their influence on the interference activity of type I-B system in different strains. When protospacer C7S1 or *Kat* gene on the plasmid were targeted, Cas6-1 supplementation in wild-type strain failed to enhance the plasmid interference activity; Cas6-1 complementation could restore the interference activity only in the absence of Cas6-2; Cas6-2 supplementation in Δ*cas6-1* strain inhibited type I-B interference; and Cas6-2 complementation in Δ*cas6-2* strain also restored the inhibition on the interference activity (Fig. 3d, e). As for chromosome targeting, Cas6-1 complementation in Δ*cas6-1* strain restored the interference activity of I-B system. And Cas6-2 supplementation or complementation did not interfere with the chromosome targeting activity in the presence of Cas6-1 (Fig. 3f). These results suggested that Cas6-2 inhibited the interference activity of type I-B system mainly when this system targeted multi-copy targets such as invading plasmids.

Occupancy of Cas6-1 by type I-B effectors attenuates utilization of Cas6-1-processed crRNA by type III effectors

The plasmid interference assays of type III CRISPR-Cas system were performed through Cas6-1 and Cas6-2 supplementation or complementation. The results showed that Cas6-1 supplementation did not affect the strong interference activity of type III system (Fig. 3g, h). Unexpectedly, Cas6-1 supplementation in Cas6-2 deletion strains restored the interference activity of type III system (Fig. 3g, h, i), implying that the crRNA processed by Cas6-1 could be utilized by type III effectors. As mentioned above, the type III system did not exhibit any interference activity in Δ*cas6-2* strain with a basal expression of *cas6-1* (Figs. 2a and 3a). Transcriptome analysis also showed that the expression level of almost all CRISPR-related genes was relatively

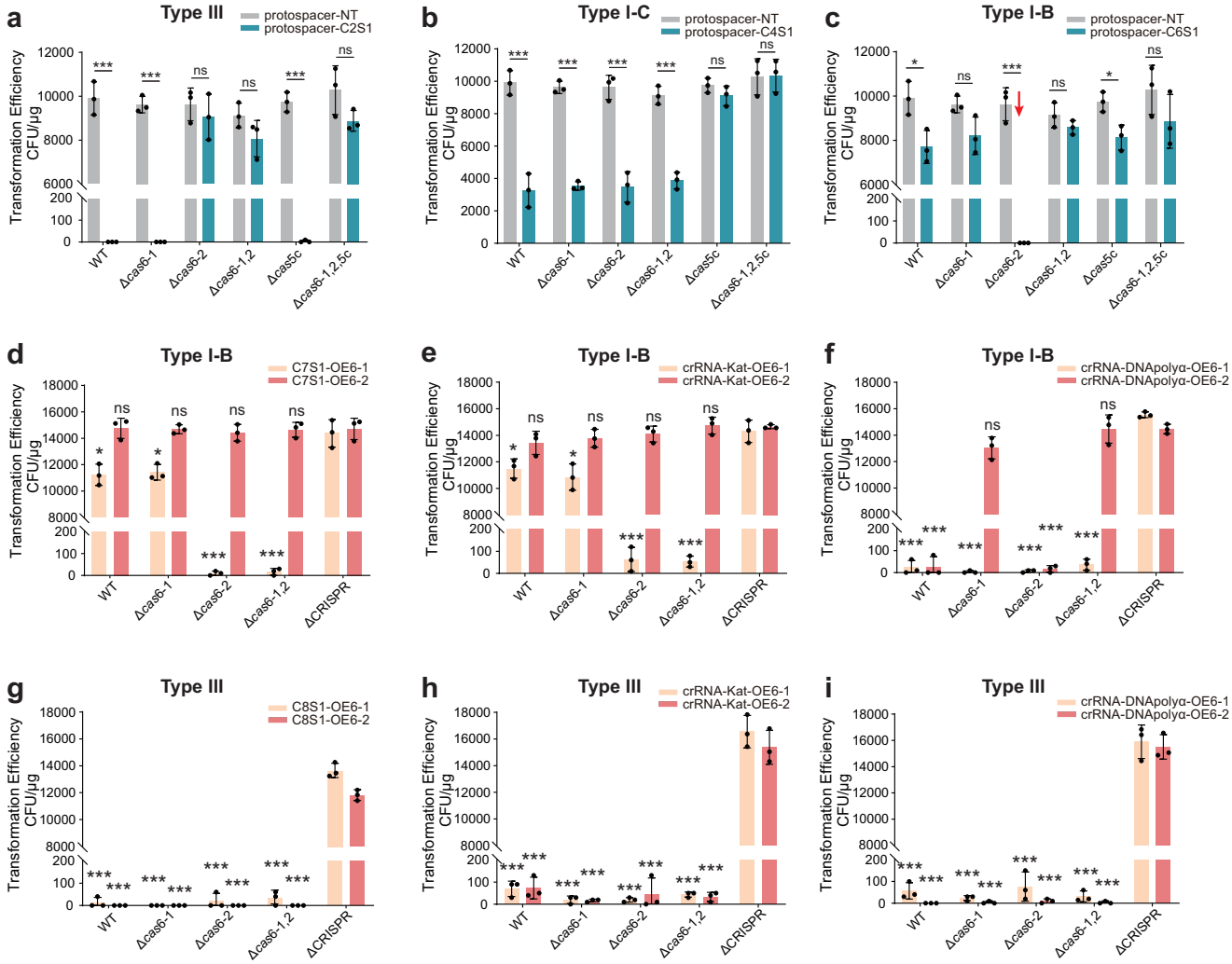

Fig. 3 | Inhibition of interference activity of the type I-B CRISPR-Cas system by Cas6-2. a, **b**, **c** Detection of interference activity in various *T. thermophilus* HB27 strains via the way of transforming invader plasmids. protospacer-C2S1/C4S1/C6S1 represents the invader plasmid carrying a target sequence of spacer 1 in CRISPR arrays 2, 4, and 6, which were used to detect the interference activity of III-AB, I-C, and I-B CRISPR-Cas systems, respectively. The red arrow indicates the enhancement of the I-B system's interference activity due to the deletion of *cas6-2*. Non-target plasmid was used as control (protospacer-NT). **d**, **e**, **f** The impact of Cas6-1 and Cas6-2 supplementation or complementation on the interference activity of type I-B systems in different *T. thermophilus* HB27 strains. **d**, **e**, **f** represent plasmids carrying protospacer (C7S1), spacer targeting resistance gene, and spacer targeting genome, respectively. Significance values indicate a significant difference from the ΔCRISPR group. **g**, **h**, **i** The impact of Cas6-1 and Cas6-2 supplementation or complementation on the interference activity of type III systems in different *T. thermophilus* HB27 strains. **g**, **h**, **i** represent plasmids carrying protospacer (C8S1), spacer targeting resistance gene, and spacer targeting genome, respectively. Significance values indicate a significant difference from the ΔCRISPR group. The data show means of three biological replicates. Error bars indicate the standard deviations (SD). Between-group significance was determined using the unpaired two-sample *t*-test (*$P < 0.05$, **$P < 0.01$, and ***$P < 0.001$). And ns indicates no significance.

low, and that Cas6-2 had about four times lower transcription levels than Cas6-1 (Supplementary Data 2). Based on these results, we speculated that when it was naturally expressed in HB27, Cas6-1 might be preferentially assembled into type I-B effector complex, and thus, Cas6-1 might not be adequate to be utilized by type III system. To confirm this speculation, we further knocked out the operon of type I-B system in Δ*cas6-2* strain, but retained only *cas6-1* gene. Plasmid interference assay showed that additional operon deletion of I-B system significantly enhanced the interference activity of type III system in Δ*cas6-2* strain (Supplementary Fig. 10), suggesting that in the operon absence of type I-B system, Cas6-1 was released to process crRNAs for type III effector complex.

Both Cas6-1 and Cas6-2 could anchor mature crRNA and interact with Cas5 subunit of type I-B effector complex in HB27

To explore how Cas6-1 and Cas6-2 function in the type I-B effector complex, we investigated the characteristics of these two crRNA-processing ribonucleases during the assembly process of I-B Cascade complex. Firstly, we examined the effects of *cas6-1* and *cas6-2* deletion on transcriptional levels of type I-B *cas* genes through RT-qPCR. The results showed that deletion of *cas6-1* and *cas6-2* genes did not significantly affect transcription level of type I-B *cas* genes (Supplementary Fig. 11). As mentioned above, Cas6-2 could process Repeat-3 of type I-B system in vivo (Supplementary Fig. 7) and in vitro (Fig. 2e). Therefore, it is of great importance to determine whether Cas6-2 remains bound to the crRNA containing Repeat-3 after cleavage and whether it can participate in the subsequent assembly of type I-B Cascade complex. By non-denaturing polyacrylamide gel assay, we found that just like many other Cas6 ribonucleases, both Cas6-1 and Cas6-2 could bind the mature crRNAs (Fig. 4a)[24,45]. Further, these two Cas6 proteins (Cas6-1 and Cas6-2) and all the proteins of type I-B system (Cas5b, Cas7b, Cas8b, and Cas3b) were expressed in *E. coli* and affinity purified, with Cas6-1 and Cas6-2 fused with a GST tag and type I-B system proteins fused with a poly-His tag (Supplementary Fig. 12). GST Pull-down assay showed that Cas6-2 and Cas6-1 only interacted with Cas5b protein of type I-B system (Fig. 4b, c),

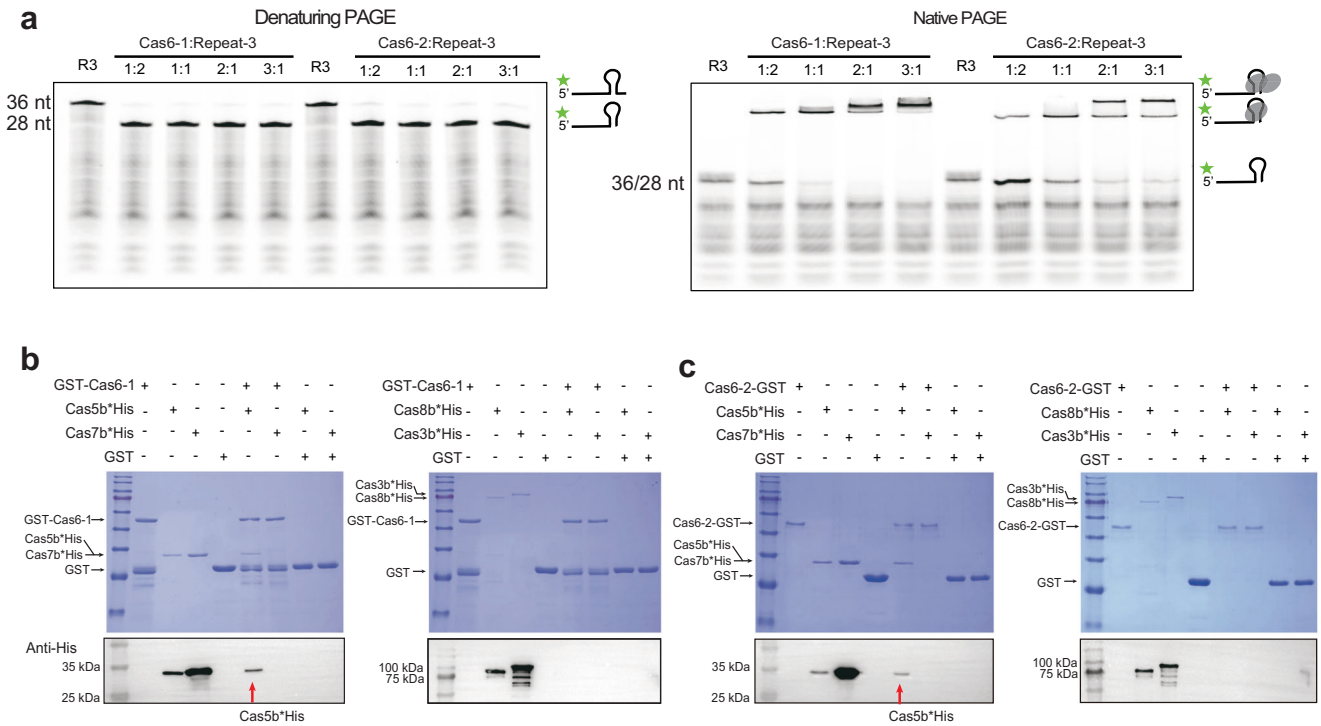

Fig. 4 | Cas6-1 and Cas6-2 both can bind their cleavage products after cleaving Repeat-3, and both exhibit protein interactions with Cas5b. a Cleavage product binding affinities of Cas6-1 and Cas6-2 to 5'-FAM labeled Repeat-3. The left panel shows the cleavage of the 5' FAM-labeled Repeat-1 by Cas6-1 and Cas6-2 in different ratios within 1 h. The right panel shows the native PAGE gel analysis after the cleavage of the 5' FAM-labeled Repeat by Cas6-1 and Cas6-2 in different ratios. R3 stands for Repeat-3. **b** GST pull-down assays of GST-Cas6-1 with various poly-His-tagged Cas proteins of the type I-B system. **c** GST pull-down assays of Cas6-2-GST with various poly-His-tagged Cas proteins of the type I-B system. Proteins are indicated by black arrows (left side). Lanes 2 to 5 represent the analysis of input samples for different proteins through SDS-PAGE and Western blotting, rather than GST pull-down assays. Lanes 6 to 9 represent the co-elution analysis from the GST pull-down assays. Interactions between the GST tag and different Cas subunits in both experimental groups were also examined to rule out non-specific interactions. Western blot assays were performed to show His-tagged proteins using the anti-His antibody. Red arrows showed the Cas5b*His protein imprinted by Western blot.

indicating that both Cas6-1 and Cas6-2 might be involved in the subsequent assembly of type I-B Cascade complex after crRNA processing.

Cas6-2 inhibits the interference activity of type I-B system by competing with Cas6-1 for assembly of type I-B Cascade complex

To explore whether Cas6-2 can participate in the assembly of type I-B Cascade complex, we purified the complex in both wild-type and Δ*cas6*-1 strains using C-terminal-His-tagged Cas8b as a bait (Fig. 5a), and designated the two obtained complexes as Cascade-WT and Cascade-Δ6-1, respectively. Both complexes had a similar elution time (~9 min) from the gel filtration column (Fig. 5b, c), suggesting their molecular weight of above 400 kDa, which was in agreement with the reported molecular weight of type I complexes[46,47]. The SDS-PAGE assay showed that the co-purified protein complexes contained all the subunits of type I-B Cascade complex with predicted sizes (Fig. 5d). Mass spectrometry also identified all the protein subunits, revealing that Cascade-WT contained Cas6-1 and Cas6-2, whereas Cascade-Δ6-1 contained only Cas6-2 (Supplementary Data 3), indicating that the complexes purified from wild-type strain were a mixture of complexes individually assembled by Cas6-1 and Cas6-2. Taken together, the above results indicated that in HB27 strain, Cas6-2 could play a role similar to Cas6-1 and participate in the assembly of the type I-B Cascade complex.

To examine the distribution of I-B Cascade-bound crRNAs in the CRISPR arrays, the crRNAs were extracted from the purified Cascade-Δ6-1 complex for high-throughput sequencing. The sequencing reads showed that the I-B Cascade-bound crRNAs originated solely from the three CRISPR arrays: CRISPR-6, CRISPR-7, and the artificial mini-CRISPR array on plasmid for Cascade purification (Fig. 5e). To investigate the maturation status of crRNAs bound to two I-B Cascade complexes, we extracted crRNAs from these two complexes and analyzed crRNA sizes. The results showed that all the extracted crRNAs exhibited the size (~70 nt) identical to that of mature crRNA in the type I-B system (Supplementary Fig. 13). Subsequently, we assessed the in vitro target cleavage activity of the two purified complexes (Fig. 5f). Cascade-WT exhibited significant cleavage activity against the non-target strand and the ATP-dependent processive degradation activity of Cas3b (Fig. 5g), which was consistent with the reported characteristics of Cas3[47,48]. Furthermore, we also found that WT-Cascade displayed an ATP-independent cleavage pattern towards the target strand, which was significantly different from ATP-dependent cleavage pattern towards the non-target strand (Fig. 5h). In contrast, Cascade-Δ6-1 exhibited no cleavage activity towards either the target or non-target strands (Fig. 5i, j), hinting that Cascade-Δ6-1 might be an inactive complex. The target binding assay confirmed that Cascade-Δ6-1 lost the ability to bind to the target dsDNA (Supplementary Fig. 14). The above results suggested that the type III-associated Cas6 protein could act as a negative regulator by competing with the I-B Cas6 protein during the assembly of type I-B Cascade complex. This competition resulted in the formation of nonfunctional effector complexes, which might alter both the structural conformation and allosteric dynamics necessary for target recognition. Consequently, the population of active Cascade complex containing Cas6-1 was diminished, ultimately attenuating the type I-B system's interference efficacy against multi-copy targets in *T. thermophilus* HB27.

Discussion

Class 1 CRISPR-Cas systems, mainly composed of type I and type III systems, account for over 90% of all discovered CRISPR-Cas systems. The co-occurrence of type I and type III systems within an organism is a widespread

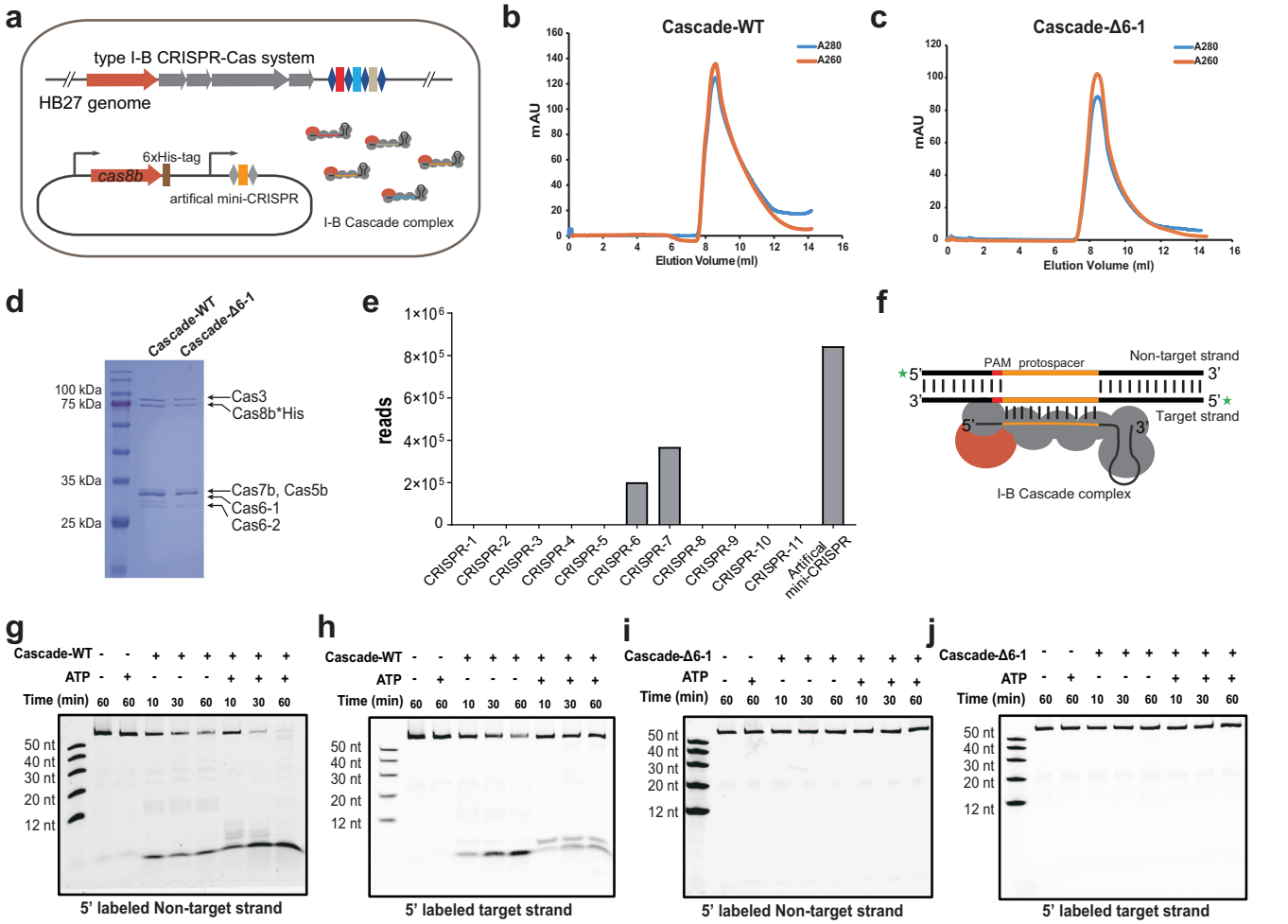

Fig. 5 | Cas6-2 can assemble with the Cas subunits of the type I-B system into an inactive Cascade complex. a Strategy for copurification of native I-B Cascade complex using pRKP31-PEDVSp3-Cas8His plasmid. **b** The SEC chromatogram of the Cascade complex purified by a C-terminal His-tagged Cas8b in the wild-type strain (Cascade-WT). **c** The SEC chromatogram of the Cascade complex purified by a C-terminal His-tagged Cas8b in the HB27Δ*cas6-1* strain (Cascade-Δ6-1). **d** The Coomassie-stained SDS-PAGE gel of Cascade complex samples, obtained by concentrating the elution peaks in (**b**, **c**). The subunits of the two Cascade complexes are indicated with arrows. **e** Histogram of the distribution of crRNAs present in I-B Cascade complex over the 11 CRISPR arrays and the artificial mini-CRISPR array. **f** Schematic of in vitro dsDNA cleavage assay of type I-B Cascade complex. The 5' FAM labeled non-target strand or target strand is shown. **g**, **h** Cleavage of dsDNA mediated by Cascade-WT complex in the absence or presence of ATP. **i**, **j** Cleavage of dsDNA mediated by Cascade-Δ6-1 complex in the absence or presence of ATP. The 5' FAM-labeled non-target strand or target strand, is indicated at the bottom of each panel. Time duration (minutes) is shown.

phenomenon, and these systems exhibit high similarity in the maturation of crRNAs and the composition of their effector complexes, suggesting their close evolutionary relationship[9]. In the case of co-occurrence of type I and type III CRISPR-Cas systems, whether there is any interaction and regulation between these two systems and whether there is synergy or interference when they exert their defensive functions remains to be investigated. crRNA is an indispensable component of CRISPR-Cas effector complex, playing a key role in the specific cleavage of targets. In this study, we first investigated the attribution of CRISPR arrays and crRNA processing proteins. The results showed that the 11 CRISPR arrays were specifically attributed to type I-B, I-C, and III-A/B CRISPR-Cas systems in HB27. This was inconsistent with previous report that in some strains, both type I and type III systems share CRISPR arrays, thus leading to simultaneous DNA and RNA targeting towards invaders[22]. By retaining different types of CRISPR arrays, HB27 is more likely to employ various CRISPR-Cas systems to defend against different types of invaders. However, the lack of thermophilic bacteriophage databases limits the exploration of the origins of spacers from CRISPR arrays. Whether each CRISPR-Cas system uses its own CRISPR array to target a specific invader or non-specifically target a general invader remains to be further investigated. In addition, we also found that type I system had a lower interference activity against multi-copy targets than type III system. The possible reason might be that type I system may serve as the first line of defense against invaders, while the delayed type III system, whose activity relies on the transcription of targets and cOA-activated Csm6/Csx1 ribonucleases, may act as a second line of defense to eliminate the escape multi-copy targets. When targeting late-expressed genes or high-copy DNA targets, the DNA-targeting systems initiate preliminary defense against exogenous DNA, with the delayed type III system serving as a subsequent supplementation[23]. One previous study has also reported that only type III system acquired new spacers from invader bacteriophages[41], indicating that type III system is an active guardian in HB27.

Although different CRISPR arrays in HB27 exhibited strict specificity among the various CRISPR-Cas systems, Cas6-1 protein of type I-B system and Cas6-2 protein of type III system were found to have cross-processing activity towards different types of crRNAs in HB27. One previous study has demonstrated that both TtCas6A (corresponding to Cas6-2 in our study) and TtCas6B (corresponding to Cas6-1) could cleave two CRISPR repeats in *T. thermophilus* HB8, and that the binding affinity of TtCas6A to two repeat cleavage products is significantly higher than that of TtCas6B[43]. In our study, Cas6-2 exhibited a higher cleavage efficiency towards Repeat-1 than Cas6-1, but Cas6-2 and Cas6-1 showed similar cleavage efficiency towards Rpeat-3

(Fig. 2d, e). This finding was consistent with our RT-qPCR results of pre-crRNA processing by two Cas6 proteins. Our data showed no increase in pre-crRNAs from type III CRISPR arrays in the absence of Cas6-1 (Supplementary Fig. 7). Therefore, although the two Cas6 proteins had high homology and cross-cleavage activity, they still displayed a certain affinity preference to different substrates. For the first time, we observed that Cas6-2 inhibited the plasmid interference activity of type I-B CRISPR-Cas system. Unexpectedly, Cas6-1 had little effect on the plasmid interference activity of type III system. Specifically, Cas6-1 supplementation in wild-type strain failed to enhance the plasmid interference of type I-B system, but Cas6-1 complementation in Δ*cas6-1,2* strain restored the interference activity of type I-B system, while Cas6-2 complementation in Δ*cas6-2* strain restored the inhibition on plasmid interference activity of type I-B system (Fig. 3d, e). These results indicated that Cas6-2 might be the main processing protein of type I and type III systems, and its high affinity even compensated for low expression of Cas6-2 in HB27. Although the absence of Cas6-1 had little effect on the interference activity of type III system, Cas6-1 supplementation in Cas6-2 deletion strains restored the interference activity of type III system. Since Cas6 is not a component of type III effector complex[30,49], Cas6-1-processed crRNA after further trimming would be assembled into the type III complex for invader defense. This suggested that when the expression level of Cas6-1 was sufficient, the Cas6-1-processed crRNAs containing Repeat-1 could be utilized by type III system, but when Cas6-1 had the natural expression, crRNAs containing Repeat-1 were mainly occupied by the I-B Cascade complex, thus attenuating their utilization by type III system.

Most Cas6 family proteins in type I CRISPR system remain bound to the processed crRNA to recruit the relevant subunit proteins so as to initiate the assembly of the complex[8]. The binding firmness of Cas6 to the processed crRNA determines whether Cas6 is a single-turnover or a multiple-turnover enzyme to some extent, and the enzymatic properties of both types of Cas6 have been reported[24,43]. In this study, we confirmed the ability of both Cas6-1 and Cas6-2 proteins to anchor the mature crRNAs, and found that both of them were multiple-turnover enzymes (Fig. 4a). After binding of Cas6 to mature crRNAs, two shift bands were observed, suggesting the formation of Cas6 dimer-crRNA complex, which was a typical phenomenon for Cas6 protein of I-B systems[15,17,18]. We also found that both Cas6-1 and Cas6-2 interacted with Cas5b subunit of type I-B system in HB27, suggesting that Cas6 mediated the assembly of the type I Cascade complex. Consistently, recent crystal structural analysis also highlighted the important role of Cas5b in the assembly of type I-B Cascade complex[28]. Based on these results, we speculated that Cas6-2 could compete with Cas6-1 of the I-B system and participate in the assembly of type I-B Cascade complex.

Type I-B Cascade complex purification and nucleic acid cleavage assays in vitro demonstrated that Cas6-2-assembled Cascade complex had no cleavage activity against DNA targets. This explained why the absence of Cas6-2 greatly enhanced the plasmid interference activity of type I-B system. In this study, the type III-associated Cas6-2 protein was able to replace the Cas6-1 protein to participate in the assembly of I-B Cascade complex, resulting in the formation of an inactive complex. This competitive effect led to partial occupancy of Cas proteins of type I-B system by Cas6-2, reducing the population of functionally active Cascade complexes and consequently impairing the defense of type I-B system against multi-copy targets. This revealed a novel mechanism by the host itself to regulate the activity of the CRISPR-Cas system, which was different from those previously reported[50,51]. In one recent study, 11 anti-CRISPR families were identified from the prophages and mobile genetic elements of *Listeria* strain. Among these 11 families, 3 anti-CRISPR proteins were found to be homologous to Cas proteins of the type I-B system in *Listeria*. For example, anti-CRISPR protein AcrIB3 was homologous to Cas5 of the I-B system, and it can replace Cas5 to participate in the assembly of the Cascade complex, thus forming an inactive complex that cannot recognize target DNA[52]. This is in line with the inhibitory mode of Cas6-2 on type I-B system in our study. Therefore, the involvement of Cas-like proteins in regulating the activity of CRISPR-Cas systems may represent a novel regulatory mechanism that has not yet been well explored, especially for the type I-B system. The crRNAs in type I-B Cascade complex of HB27 were derived only from the Repeat-3-carrying CRISPR arrays unique to type I-B system, indicating that type I-B system could not use the processed crRNA from type III CRISPR arrays to assemble complex. The type III system utilizing Repeat-3 exhibited no interference activity. The possible reason might be that type III effector complex can not be assembled, or that the assembled complex is non-functional, which remains to be further investigated. It has been reported that crRNAs from type I and type III CRISPR arrays can be further processed to form smaller crRNA without the 3' stem loop in HB8[42]. It seems that the type III Cas proteins can load Cas6-1/Cas6-2-processed crRNA carrying Repeat-3 to form a type III effector complex. However, crRNAs extracted from TtCsm and TtCmr complexes are derived only from type III CRISPR arrays in HB8[30,49]. The 3' trimming of Cas6-processed crRNA and complex assembly of type III system need further investigation. Notably, our data showed that Cas3 in HB27 and Cascade complex were co-purified in an R-loop formation-independent manner, which was in accordance with previous study findings of some type I-A and I-G systems[29,53], but inconsistent with one recent report on crystal structure analysis of type I-B system in *Synechocystis sp*. PCC 6714[28]. The reason for the difference might be attributed to the diversity of Cascade complexes of type I-B systems.

Currently, the crystal structures of various type I and type III CRISPR effector complexes have been determined, yet the dynamic assembly processes of these complexes remain poorly understood. Cas6, frequently serving as the initiating protein for the assembly of type I and III complexes, plays a critical role in this process. Integrating the findings of this study, we propose a putative model for crRNA processing and CRISPR effector complex assembly of type I-B and type III systems in *T. thermophilus* HB27 (Fig. 6). For the type I-B CRISPR-Cas system, both Cas6-1 and Cas6-2 proteins can competitively recognize and bind to pre-crRNAs, and both recruit Cas5b through protein-protein interactions. Furthermore, we propose that the interaction between Cas6 and Cas5b may represent a weak or transient binding event. After Cas6-mediated cleavage of the repeat sequence, Cas6 proteins remain associated with the 3'-stem-loop structure of the crRNA, while Cas5b localizes to the 5'-handle region. Subsequently, other Cascade subunits are recruited by unknown mechanisms, ultimately forming the complete Cascade complex. However, the Cascade complex assembled with Cas6-2 protein is inactive, thereby regulating the activity of type I-B CRISPR-Cas system in *T. thermophilus* HB27. In contrast, for the type III system, since Cas6 is not a component of its effector complex, Cas6 proteins dissociate from the type III crRNAs after cleaving the repeat sequence. Subsequently, the 3'-stem-loop structure of the crRNA is trimmed by unknown processing proteins, and relevant Cas proteins might be recruited through its specific 5'-handle sequence, ultimately completing the assembly of the type III effector complex. Our findings, particularly the elucidation of interactions between Cas6 and Cas5, provide critical insights into understanding the dynamic assembly processes of type I and type III CRISPR effector complexes. It is worth noting that although Cas6 and Cas7 are often found in close proximity within the Cascade complex, we did not detect direct interaction between these two proteins through pull-down assays. This suggests that Cas7 may be recruited through features of the crRNA sequence or other mechanisms. We also conducted a phylogenetic analysis of Cas6 proteins from different strains (Supplementary Fig. 15), showing that Cas6-1 was distantly related to some type I-B Cas6 proteins but closely related to Cas6-2 and some type III Cas6 proteins. This suggests that different types of Cas6 proteins may share functional similarities. Additionally, the structural comparison of Cas6-1 and Cas6-2 revealed high similarity, which partly explains their interactions with Cas5b and involvement in Cascade complex assembly. Furthermore, structural studies of the inactivated Cascade complex, such as cryo-EM or mutagenesis studies, will help further elucidate the mechanism by which Cas6-2 disrupts the Cascade activity. We will pursue these approaches in our future research to advance the understanding of this process.

Although CRISPR immunity provides protection against phages, increasing evidence indicates that highly active CRISPR-Cas systems

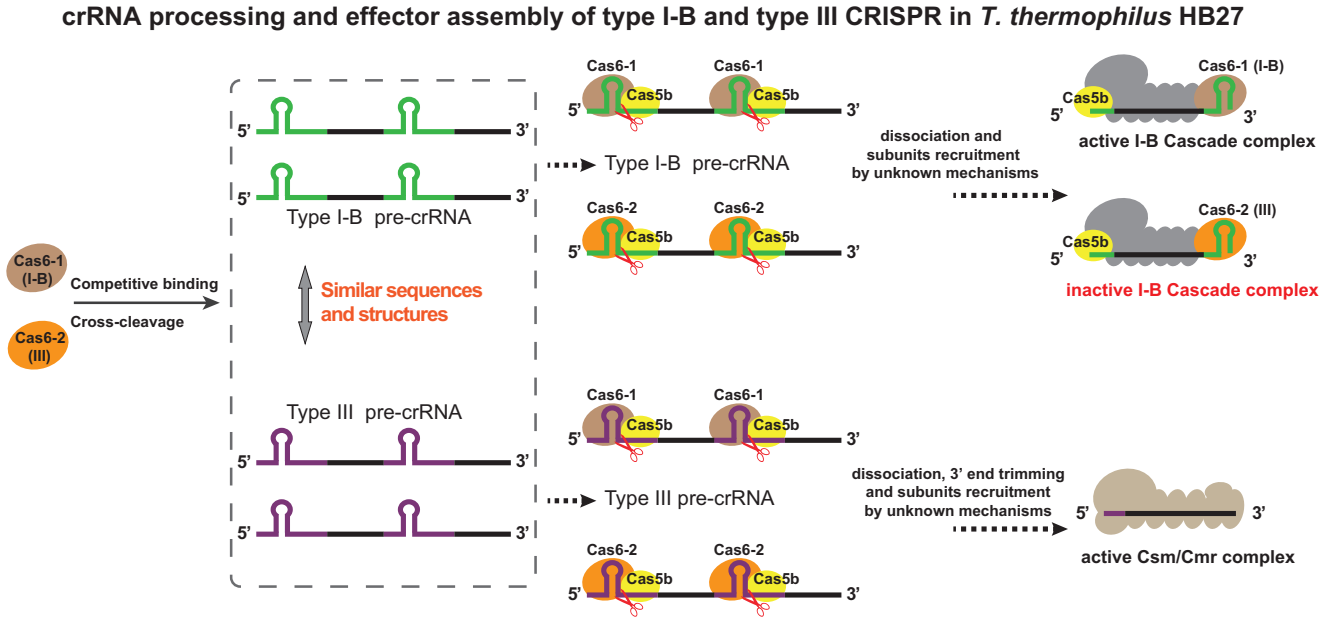

Fig. 6 | A putative model for crRNA processing and CRISPR effector complex assembly of type I-B and type III systems in *T. thermophilus* HB27.

impose a significant burden on the host[54–56]. For example, CRISPR-Cas system repels beneficial elements, incurs expression costs, and poses the risk of self-targeting. To alleviate these burdens, some bacterial endogenous CRISPR-Cas systems are often in a state of self-inhibition[57–60]. Our transcriptome analysis of HB27 revealed that the transcription levels of four different endogenous subtypes of the CRISPR-Cas systems were relatively low (Supplementary Data 2), which may be a strategy adopted by HB27 to reduce the burdens brought by CRISPR systems. Although Cas6-2 inhibited the interference activity of type I-B CRISPR system in vivo, it might play an important role in maintaining the normal physiological state of HB27 by reducing the risk of self-targeting.

In summary, for the first time, our study reported multiple biological functions of co-occurrence and cross-cleavage of different Cas6 proteins in a multi-CRISPR system, including crRNA processing, effector complex assembly, and target interference. Our results provide an insight into the functions of type I and type III CRISPR-Cas systems and reveal the complex regulatory mechanisms underlying different CRISPR systems. Elucidation of the interaction between Cas6 and Cas5 proteins by us will also provide key insights into the molecular mechanisms driving the dynamic assembly of Cascade complexes. Our findings may also offer new insights for designing gene editing tools based on the type I-B CRISPR-Cas system of HB27 and improving their precision by regulating Cas6-2 expression with inducible promoters or optogenetic switches.

Material and methods

Strains, culture conditions, and transformation

Strains and plasmids used in this study are detailed in Supplementary Table 1. *T. thermophilus* HB27 and the derived stains were cultured at 65°C in the modified TB medium[38]. *Escherichia coli* strains DH5α and BL21 (DE3) were used for plasmid construction and protein expression, respectively, and they were cultured at 37 °C in Luria-Bertani medium.

Transformation of the *T. thermophilus* was conducted as a natural transformation method with some modifications[38]. In brief, the overnight HB27 culture was inoculated into fresh TB medium at 4% and incubated with shaking at 65 °C for 2.5 h. The culture (1 mL) was then mixed with 500 ng of plasmid and incubated with shaking at 65 °C for an additional 2.5 h. Subsequently, 200 µL of the bacterial suspension was spread on selective plates. When assessing the interference activity of the type I-B system against exogenous plasmids, to facilitate colony counting, only 100 µL of the bacterial suspension was spread on the plates. For the *T. thermophilus* and *E. coli* strains containing kanamycin-resistant plasmids, kanamycin was added to their culture media at final concentrations of 20 µg/mL and 30 µg/mL, respectively. For the *E. coli* strains containing ampicillin-resistant plasmids, ampicillin was added to their culture media at final concentrations of 100 µg/mL.

Construction of gene-deletion strains

The construction of all gene-deletion strains of *T. thermophilus* HB27 was based on the methods we previously reported[38]. The gene-editing plasmids were constructed based on a shuttle vector carring a P31 promoter and an artificial mini-CRISPR array named pRKP31-AC. The spacer fragment of mini-CRISPR array was generated by annealing of the corresponding complementary oligonucleotides (Supplementary Table 2) and inserted into pRKP31-AC at the Bbs I sites. The donor DNA fragments containing a mutant allele of each target gene were generated by splicing and overlap extension PCR and subsequently inserted into corresponding constructs using a seamless cloning kit (Abclonal, Wuhan, China). Each gene-editing plasmid was introduced into *T. thermophilus* HB27 by a natural transformation method[61]. Transformants were screened by PCR validation using primers listed in Supplementary Table 2. The resulting PCR products were analyzed by agarose gel electrophoresis and DNA sequencing (Sangon, Shanghai, China). And the editing plasmid was eliminated through subculturing without antibiotics.

Construction of interference activity validation plasmids

The interference activity validation plasmid was composed of two types: one type was called the interference plasmid, containing a self-targeting mini-CRISPR array, and the other was the invader plasmid, carrying the protospacer sequence. The pRKP31-AC was used to construct a series of interference plasmids derived from our previous studies[38]. Firstly, the plasmid was linearized by the restriction enzyme at its Bbs I sites. Subsequently, a spacer fragment containing sticky ends formed by annealing of two complementary oligonucleotides is ligated to this linearized vector. For the construction of invader plasmids, the protospacer sequences designed based on the CRISPR arrays in the HB27 genome were inserted into the linearized vector pRKP31, which was derived from the pRKP31-AC with deletion of the artificial mini-CRISPR array. All the plasmids were confirmed by sequencing before transformation. All oligonucleotides (Supplementary Tables 2 and 3) were synthesized in Sangon, Shanghai, China. Restriction enzymes and ligase were purchased from Thermo Fischer Scientific, Waltham, MA, USA.

Total RNA extraction and reverse transcriptase with quantitative polymerase chain reaction

For the extraction of the total RNA of different HB27 strains, overnight cultured HB27 strains were subcultured at a ratio of 2% and cultured to an optical density at 600 nm (OD_{600nm}) of ~0.5. Then, 3 mL of fresh bacterial culture was used for the extraction of total RNA. Total RNA samples used for reverse transcriptase with quantitative polymerase chain reaction (RT-qPCR) analysis were extracted using RNA-easy Isolation Reagent (Vazyme, Nanjing, China) according to the manufacturer's instructions. Then 1 μg RNA was used for generating complementary DNA (cDNA) with ABScript III RT Master Mix for qPCR with gDNA Remover (Abclonal, Wuhan, China) using random primer in a 20-μL volume. And residual genomic DNA in the total RNA sample is also eliminated at this step. The cDNA obtained was used for qPCR. A chromosomally located, constitutively expressed gene (*TT_C1610*) was chosen as an endogenous ref.[62]. PCR was performed using Universal SYBR Green Fast qPCR Mix (Abclonal, Wuhan, China) and a QuantStudio 3 Real-Time PCR System (Applied Biosystem) with the following PCR condition: denaturing at 95 °C for 3 min, 40 cycles of 95 °C for 5 s, 60 °C for 34 s. Primers used were listed in Supplementary Table 2. The nucleic acid extraction and reaction setup processes were both carried out on ice to ensure the integrity of the RNA. To ensure the accuracy of the data, the experiments were conducted with three biological and technical replicates. The relative quantification method ($2^{-\Delta\Delta CT}$) was used in the calculations.

Extraction of genomic DNA and determination of the relative copy number of plasmid and chromosomal DNA

For the extraction of the genome DNA of *T. thermophilus*, overnight cultured HB27 strains were subcultured at a ratio of 2% and cultured to an optical density at 600 nm (OD_{600nm}) of ~1.0. Then, 5 mL of cell culture was collected by centrifugation. The cell pellet was resuspended in 300 μL of TES buffer (10 mM Tris-HCl (pH 8.0), 1 mM EDTA, 0.5% (m/v) SDS, 20 μg/mL of Proteinase K) and incubated at 55 °C for 30 min. Subsequently, the sample was extracted using the DNA extraction reagent (Phenol: Chloroform: Isoamyl alcohol = 25:24:1 (pH > 7.8)). Nucleic acids from the aqueous phase were ethanol precipitated in the presence of 1/10 volume of 3 M sodium acetate (pH 5.2). After centrifugation, the resulting pellet was washed twice with 70% cold ethanol, dried at room temperature, and resuspended in double-distilled water. qPCR analysis of *TT_C1610* (genome DNA) and *puc-ori* (plasmid DNA) was carried out as described above. Plasmid per genome ratio was calculated based on normalized (with primer efficiency) ratio of *puc-ori* and *TT_C1610* qPCR signals. To ensure the accuracy of the data, the experiments were conducted with three biological and technical replicates.

Transcriptome sequencing

Cells from 20 mL of *T. thermophilus* HB27 culture ($OD_{600} = 0.5$) were harvested by centrifugation. Then, total RNA was extracted from the cells using the TRI Reagent (Sigma-Aldrich) according to the instructions provided by the manufacturer. The obtained RNA samples were treated with RNase-free DNase I (Thermo Fisher Scientific). Biological triplicates of purified RNA were sequenced by Sangon (Shanghai, China) by Illumina sequencing. The raw data from sequencing were assessed for quality using FastQC tool. Adaptor trimming was performed using Trimmomatic V0.36[63]. Processed reads were mapped to the reference sequences using bowtie2 V2.32 with default setting[64]. Based on the alignment results, RSeQC V2.61 was utilized to carry out analyzes of redundant sequences and the distribution of insertion fragments[65]. FeatureCounts V1.6 and the known gene model were used to assess gene expression levels[66]. TPM (transcripts per million) values were calculated with normalization on a total number of counted reads.

Construction of *Escherichia coli* expression plasmids and strains

For the expression of His-tagged proteins in *E. coli*, pET28a-HRV3C was used. The coding sequences of Cas6-1, Cas5c, Cas6-2, Cas5b, Cas7b, Cas8b, and Cas3b were amplified from the genomic DNA of *T. thermophilus* HB27 by PCR using the primers listed in Supplementary Table 2. Then the gene fragment was inserted into pET28a-HRV3c between the Nco I and Xho I restriction sites to generate C-terminal 6× His tagged proteins. For the expression of GST-tagged proteins in *E. coli*, pGEX-6p-1 was used. *cas6-1* and *cas6-2* were amplified from the genomic DNA of by PCR. The *cas6-1* gene fragment was inserted into pGEX-6p-1 between the BamH I and Sal I restriction sites to generate an N-terminal GST-tagged Cas6-1. For Cas6-2, when an N-terminal GST tag was fused, the fusion protein exhibited very low solubility. Therefore, we fused the GST tag to the C-terminus of Cas6-2 by Gibson assembly method. All the plasmids were confirmed by sequencing before transformation and then transformed to *E. coli* BL21 (DE3) to obtain corresponding strains.

Protein expression and purification

To express His-tagged Cas6-1, Cas6-2, Cas5c, Cas5b, Cas7b, Cas8b, and Cas3b from *E. coli* BL21 (DE3), the strains carrying the indicated plasmids were grown in LB medium containing the corresponding antibiotics at 37 °C. When the cells were cultured to an optical density at 600 nm (OD_{600nm}) of ~0.8, protein expression was induced with 0.5 mM isopropyl-β-d-thiogalactopyranoside (IPTG) at 18 °C for 18 h. Then, cells were pelleted by centrifugation at 7000 × *g* for 10 min. The cell pellet collected from 1 L of culture was resuspended in 40 mL of lysis buffer (20 mM HEPES, pH 7.5, 300 mM NaCl, and 5% (v/v) glycerol). Cells were disrupted by French press, and debris was removed by centrifugation at 15,000 × *g* and 4 °C for 30 min. Then the cell extract was loaded onto Ni-charged Resin FF columns (GenScript, Nanjing, China). After the column was washed with lysis buffer containing 50 mM imidazole, His-tagged proteins were eluted with lysis buffer containing a series of gradient concentrations of imidazole (100, 200, 500, 1000 mM). The fractions containing target proteins were concentrated employing an Amicon Ultra centrifugal filter with the corresponding cutoff (Millipore, Billerica, MA, USA) and then loaded onto a Superdex 200 Increase 10/300 GL column (Cytiva, Marlborough, MA, USA). The proteins were eluted with buffer B (20 mM HEPES, pH 7.5, 300 mM NaCl) and analyzed by sodium dodecyl sulfate–polyacrylamide gel electrophoresis (SDS–PAGE). Finally, The fractions containing target proteins were concentrated again and aliquoted for storage at -80°C.

To express GST, GST-tagged Cas6-1 and Cas6-2 from *E. coli* BL21 (DE3), the strains are cultured, harvested, and disrupted as described before. Then the cell extract was loaded onto GST-Sefinose Resin 4FF columns (Sangon, Shanghai, China) pre-equilibrated with phosphate buffer (140 mM NaCl, 2.7 mM KCl, 10 mM Na_2HPO_4, 1.8 mM KH_2PO_4, pH 7.4). After the column was washed with phosphate buffer, GST-tagged proteins were eluted using an elution buffer (phosphate buffer supplemented with 10 mM reduced glutathione, pH 8.0). The fractions containing target proteins were concentrated employing an Amiconultra centrifugal filter with corresponding cutoff (Millipore, Billerica, MA, USA) and then loaded onto a Superdex 200 Increase 10/300 GL column (Cytiva, Marlborough, MA, USA). The proteins were eluted with buffer B and analyzed by SDS–PAGE. Finally, the fractions containing target proteins were concentrated again and aliquoted for storage at -80°C.

To purify the Cascade complex of the type I-B system in *T. thermophilus* HB27, a plasmid carrying an I-B mini-CRISPR array and an expression cassette for Cas8b with His tag was transformed into HB27 (Fig. 5a). The strains carrying the indicated plasmids were grown in TB medium containing 20 μg/mL kanamycin at 65 °C for about 24 h. And cells were pelleted from at least 10 L of culture by centrifugation at 7000 × *g* for 10 min. The cell pellet was re-suspended in Buffer C (20 mM HEPES pH 7.5, 30 mM Imidazole, 500 mM NaCl) and disrupted by a French press. Cell debris was removed by centrifugation at 15000 × *g* and 4 °C for 30 min. Then the cell extract was loaded onto a 5 mL HisTrap HP column (Cytiva, Marlborough, MA, USA). After the column was washed with buffer containing 50 mM Imidazole, the Cascade complex was eluted with buffer containing 500 mM Imidazole. Fractions containing the target protein were concentrated and further purified by size exclusion chromatography (SEC)

in Buffer B, using a Superdex 200 Increase 10/300 GL column (Cytiva, Marlborough, MA, USA). Sample fractions collected during SEC were analyzed by SDS-PAGE, and those containing the complete set of Cascade complex were pooled together and concentrated again, which are aliquoted for storage at −80 °C. The protein concentration was determined by the Bradford Protein Assay Reagent (Tiangen, Beijing, China).

Small RNA sequencing analysis of Cascade-bound crRNAs

Cascade-bound crRNAs were isolated from the endogenous Cascade complex by phenol-chloroform isoamyl alcohol extraction and ethanol precipitation. The strand-specific RNA-seq library was prepared according to the directional mRNA-seq library preparation protocol provided by Illumina. Briefly, 3' and 5' adaptors were ligated to the 3' and 5' ends of small RNA, respectively. Then the first strand cDNA was synthesized after hybridization with reverse transcription primer. The double-stranded cDNA library was generated through PCR enrichment. After purification and size selection, libraries were ready for sequencing. After the library construction is completed, we performed quantification of the inserted fragments and determined the effective concentration to ensure the quality of the library. The qualified libraries were pooled and sequenced on Illumina platforms. The original fluorescence image files obtained from Illumina platform are transformed to short reads (Raw data) by base calling, and these short reads are recorded in FASTQ format[67], which contains sequence information and corresponding sequencing quality information. Raw data (raw reads) of fastq format were first processed through fastp software. In this step, clean data (clean reads) were obtained by removing reads containing adapters and low-quality reads from raw data. At the same time, Q20, Q30, and GC content the clean data were calculated. All the downstream analyzes were based on clean data with high quality. Mapping of the adaptor-stripped reads to the genome *T. thermophilus* HB27 and Cascade purification plasmid was performed with Bowtie2 using the default settings[64].

RNase cleavage assays with synthetic RNA oligonucleotides and in vitro transcripts

The 5' end FAM-labeled Repeat-1, Repeat-2, and Repeat-3 fragments were synthesized by Sangon, Shanghai, China (Supplementary Table 3). In vitro transcription of mini-CRISPR arrays of type III and I-B systems was performed with the TranscriptAid T7 High Yield Transcription Kit (Thermo Fischer Scientific, Waltham, MA, USA) according to the manufacturer's instructions. Cleavage reactions were performed in a volume of 10 μL in cleavage buffer (20 mM Tris-HCl pH8.0, 250 mM KCl, 1 mM dithiothreitol). The reaction mixture contains 1 μM Cas6 or Cas5c and the indicated concentration of 5'-labled Repeats or in vitro transcripts. The reaction was performed at 65℃ and stopped at the indicated time point by the addition of 2× RNA loading dye (NEB) and cooling on ice. Finally, the samples were heated for 10 min at 95 °C and separated on denaturing 7 M urea 15% or 8% polyacrylamide gels. For FAM-labeled substrates, gels were visualized by fluorescence imaging using a Typhoon FLA 7000 laser scanner (GE Healthcare). For in vitro transcribed substrates, gels were first stained with SYBR Green II and then visualized using a gel imaging system (Clinx, Shanghai, China).

Electrophoretic mobility shift assay

To analyze the affinity of Cas6-1 and Cas6-2 for the cleavage products of the Repeat, after conducting the cleavage assays described above, the reaction samples were subjected to non-denaturing gel analysis. For both analyzes, the concentration of the substrates was fixed as 500 nM, while the concentrations of proteins varied as indicated in the figure legends. After incubation, the reaction samples were mixed with 10× EMSA/Gel-shift loading dye (Beyotime, Shanghai, China) and separated on 12% native polyacrylamide gels. Electrophoresis was carried out under 200 V for 40 min in 0.5× TBE buffer, with the buffer maintained at 4 °C. Finally, gels were visualized by fluorescence imaging using a Typhoon FLA 7000 laser scanner (GE Healthcare). To analyze the affinity of the Cascade complex for dsDNA substrate. Cascade-WT or Cascade-Δ6-1 was incubated with the 5' FAM-labeled dsDNA at 65 °C for 1 h. The incubation buffer contained 20 mM HEPES, 100 mM KCl, 1 mM DTT. For both analyzes, the concentration of dsDNA substrates was fixed as 500 nM, while the concentrations of proteins varied as the form of a gradient increase. After incubation, the reaction samples were mixed with 10× EMSA/Gel-shift loading dye (Beyotime, Shanghai, China) and separated on 8% native polyacrylamide gels. Electrophoresis was carried out under 200 V for 40 min in 0.5× TBE buffer, with the buffer maintained at 4 °C. Finally, gels were visualized by fluorescence imaging using a Typhoon FLA 7000 laser scanner (GE Healthcare).

Pull-down assay

To explore the protein interactions between these two Cas6 and other subunits of the type I-B system, His-tagged Cas5b, Cas7b, Cas8b, or Cas3b were incubated with GST-Cas6-1, Cas6-2-GST, and GST, respectively, in 500 μL phosphate buffer (140 mM NaCl, 2.7 mM KCl, 10 mM Na_2HPO_4, 1.8 mM KH_2PO_4, pH 7.4) at 4 °C for 5 h. Subsequently, 50 μL of GST-Sepharose Resin 4FF was added to the protein mixture, and the reaction system was incubated under slow rotation at 4 °C for 1.5 h. After the incubation, the resin beads were washed three times with phosphate buffer. Finally, the resin beads were washed with 50 μL of phosphate buffer containing 10 mM reduced glutathione (pH 8.0). The supernatant samples were boiled in loading buffer, and the pulled-down protein complexes were separated on two 12% SDS-PAGE gels, one for Coomassie staining and the other for Western blot detection.

Western blot

Following electrophoresis, proteins from SDS-PAGE gels were transferred onto a PVDF membrane (pore size 0.45 μm, Millipore). The wet transfer was performed in a transfer tank with a constant current of 160 mA at 4 °C for 45 min. Post-transfer, the PVDF membrane was blocked with 6% (w/v) skim milk in phosphate buffer for 1 h at room temperature to prevent non-specific binding. The membrane was then incubated with anti-His serum (Abclonal, Wuhan, China, cat. # AE003-1:10000). After incubation with the primary antibody, the membrane was washed three times for 10 min each with phosphate buffer containing 0.1% Tween 20 (PBST) to remove unbound antibodies. Subsequently, the membrane was incubated with a horseradish peroxidase-conjugated secondary antibody (Goat Anti-Mouse IgG) (Abclonal, Wuhan, China, cat. # AS003-1:5000) for 1 h at room temperature. After removing unspecific binding, the immunoreactive bands were visualized using an enhanced chemiluminescence (ECL) detection kit (Abclonal, Wuhan, China) according to the manufacturer's instructions using Tanon 5200 (Tanon, Shanghai, China).

LC-MS/MS analysis

Mass spectrometry identification was conducted on the Cascade complex purified from different strains to determine the protein composition of the complex. All samples were analyzed on an UltiMate 3000 RSLCnano system coupled on-line with Q Exactive HF mass spectrometer through a Nanospray Flex ion source (Thermo Fischer Scientific, Waltham, MA, USA)[68]. Peptide samples were injected into a C18 Trap column (75 μm × 2 cm, 3 μm particle size, 100 Å pore size), and separated in a reversed-phase C18 analytical column packed in-house with ReproSil-Pur C18-AQ resin (75 μm × 25 cm, 1.9 μm particle size, 100 Å pore size). Mobile phase A (0.1% formic acid, 3% DMSO) and mobile phase B (0.1% formic acid, 3% DMSO, 97% ACN) were used to establish the separation gradient at a flow rate of 300 nL/min. The MS was operated in DDA top20 mode with a full scan range of 350–1500 m/z. AGC Target value for the full MS scan was 3E6 charges with a maximum injection time of 30 ms and a resolution of 60,000 at m/z 200. Precursor ion selection window was kept at 1.4 m/z, and fragmentation was achieved by higher-energy collisional dissociation (HCD) with a normalized collision energy of 28. Fragment ion scans were recorded at a resolution of 15,000, an AGC of 1E5, and a maximum fill time of 50 ms. Dynamic exclusion was enabled and set to 30 s. MS raw data were analyzed

with MaxQuant (1.6.6.0) using the Andromeda database search algorithm[69]. Spectra files 0 were searched against the *Thermus thermophilus* HB27 protein sequence database downloaded from Uniprot[70].

dsDNA cleavage assay with the Cascade complex

FAM-labeled dsDNA targets were generated by PCR using one 5' FAM-labeled primer and the other unlabeled primers (Supplementary Tables 2 and 3), and recovered by ethanol precipitation. dsDNA cleavage assays were conducted in 10 μL of reaction containing 0.1 mg/mL I-B Cascade complex purified from wild-type HB27 or HB27Δcas6-1 and 1 μM dsDNA substrate (target strand or non-target strand labeled) in the cleavage buffer (20 mM HEPES, 10 mM $MgCl_2$,100 mM KCl, 1 mM DTT) at 65 °C for 1 h or for a different time span as indicated. If required, the concentration of ATP added is 1 mM. Reactions were stopped by adding 10 μL 2× RNA loading dye (New England Biolabs). Before electrophoresis, samples were heated for 10 min at 95 °C. Then the samples are analyzed on denaturing 7 M urea 15% polyacrylamide gels. Results were visualized by fluorescence imaging using a Typhoon FLA 7000 laser scanner (GE Healthcare).

Statistics

All the histogram drawings and statistical analysis were completed by the software GraphPad Prism 8 (GraphPad Software Inc.). Data are expressed as the mean ± standard deviation (SD). Between-group significance was determined using the unpaired two-sample *t*-test ($^*P < 0.05$, $^{**}P < 0.01$, and $^{***}P < 0.001$). The number of replicates is listed in relevant figure legends.

Reporting summary

Further information on research design is available in the Nature Portfolio Reporting Summary linked to this article.

Data availability

Transcriptome and crRNA sequencing data have been deposited with the National Center for Biotechnology Information Sequence Read Archive under BioProject ID PRJNA1181933 and PRJNA1181636. The mass spectrometry proteomics data have been deposited to ProteomeXchange via the PRIDE database with identifier PXD060923 (Token: 3fq1iTIawm10). Source data for graphs is provided as Supplementary Data 1. Uncropped and unedited blot images are provided as Supplementary Figs. 16–18. All other data are available from the corresponding authors upon reasonable request.

Received: 6 March 2025; Accepted: 14 May 2025;
Published online: 23 May 2025

References

1. Barrangou, R. et al. CRISPR provides acquired resistance against viruses in prokaryotes. *Science* **315**, 1709–1712 (2007).
2. Barrangou, R. & Horvath, P. A decade of discovery: CRISPR functions and applications. *Nat. Microbiol.* **2**, 17092 (2017).
3. Marraffini, L. A. CRISPR-Cas immunity in prokaryotes. *Nature* **526**, 55–61 (2015).
4. Nussenzweig, P. M. & Marraffini, L. A. Molecular mechanisms of CRISPR-Cas immunity in bacteria. *Annu. Rev. Genet.* **54**, 93–120 (2020).
5. Koonin, E. V., Makarova, K. S. & Zhang, F. Diversity, classification and evolution of CRISPR-Cas systems. *Curr. Opin. Microbiol.* **37**, 67–78 (2017).
6. Makarova, K. S. et al. Unprecedented diversity of unique CRISPR-Cas-related systems and Cas1 homologs in asgard archaea. *Crispr. J.***3**, 156–163 (2020).
7. Altae-Tran, H. et al. Uncovering the functional diversity of rare CRISPR-Cas systems with deep terascale clustering. *Science* **382**, eadi1910 (2023).
8. Hille, F. et al. The biology of CRISPR-Cas: backward and forward. *Cell* **172**, 1239–1259 (2018).
9. Makarova, K. S. et al. An updated evolutionary classification of CRISPR-Cas systems. *Nat. Rev. Microbiol.* **13**, 722–736 (2015).
10. Hatoum-Aslan, A., Maniv, I. & Marraffini, L. A. Mature clustered, regularly interspaced, short palindromic repeats RNA (crRNA) length is measured by a ruler mechanism anchored at the precursor processing site. *Proc. Natl. Acad. Sci. USA* **108**, 21218–21222 (2011).
11. Carte, J., Wang, R., Li, H., Terns, R. M. & Terns, M. P. Cas6 is an endoribonuclease that generates guide RNAs for invader defense in prokaryotes. *Genes Dev.* **22**, 3489–3496 (2008).
12. Carte, J., Pfister, N. T., Compton, M. M., Terns, R. M. & Terns, M. P. Binding and cleavage of CRISPR RNA by Cas6. *RNA* **16**, 2181–2188 (2010).
13. Punetha, A., Sivathanu, R. & Anand, B. Active site plasticity enables metal-dependent tuning of Cas5d nuclease activity in CRISPR-Cas type I-C system. *Nucleic Acids Res.* **42**, 3846–3856 (2014).
14. Nam, K. H. et al. Cas5d protein processes pre-crRNA and assembles into a cascade-like interference complex in subtype I-C/Dvulg CRISPR-Cas system. *Structure* **20**, 1574–1584 (2012).
15. Shao, Y. & Li, H. Recognition and cleavage of a nonstructured CRISPR RNA by its processing endoribonuclease Cas6. *Structure* **21**, 385–393 (2013).
16. Richter, H. et al. Characterization of CRISPR RNA processing in Clostridium thermocellum and Methanococcus maripaludis. *Nucleic Acids Res.* **40**, 9887–9896 (2012).
17. Richter, H., Lange, S. J., Backofen, R. & Randau, L. Comparative analysis ofCas6b processing and CRISPR RNA stability. *RNA Biol.* **10**, 700–707 (2013).
18. Reeks, J. et al. Structure of a dimeric crenarchaeal Cas6 enzyme with an atypical active site for CRISPR RNA processing. *Biochem. J.* **452**, 223–230 (2013).
19. Makarova, K. S., Wolf, Y. I. & Koonin, E. V. Classification and Nomenclature of CRISPR-Cas Systems: Where from Here?. *Crispr. J.* **1**, 325–336 (2018).
20. Makarova, K. S. et al. Evolutionary classification of CRISPR-Cas systems: a burst of class 2 and derived variants. *Nat. Rev. Microbiol*. https://doi.org/10.1038/s41579-019-0299-x (2019).
21. Silas, S. et al. Type III CRISPR-Cas systems can provide redundancy to counteract viral escape from type I systems. *Elife* **6**, https://doi.org/10.7554/eLife.27601 (2017).
22. Vink, J. N. A., Baijens, J. H. L. & Brouns, S. J. J. PAM-repeat associations and spacer selection preferences in single and co-occurring CRISPR-Cas systems. *Genome. Biol.* **22**, 281 (2021).
23. Pyenson, N. C. & Marraffini, L. A. Type III CRISPR-Cas systems: when DNA cleavage just isn't enough. *Curr. Opin. Microbiol.* **37**, 150–154 (2017).
24. Sokolowski, R. D., Graham, S. & White, M. F. Cas6 specificity and CRISPR RNA loading in a complex CRISPR-Cas system. *Nucleic Acids Res.* **42**, 6532–6541 (2014).
25. Nickel, L. et al. Cross-cleavage activity of Cas6b in crRNA processing of two different CRISPR-Cas systems in Methanosarcina mazei Go1. *RNA Biol.* **16**, 492–503 (2019).
26. Reimann, V. et al. Specificities and functional coordination between the two Cas6 maturation endonucleases in Anabaena sp. PCC 7120 assign orphan CRISPR arrays to three groups. *RNA Biol.* **17**, 1442–1453 (2020).
27. Jore, M. M. et al. Structural basis for CRISPR RNA-guided DNA recognition by Cascade. *Nat. Struct. Mol. Biol.* **18**, 529–536 (2011).
28. Lu, M. et al. Structure and genome editing of type I-B CRISPR-Cas. *Nat. Commun.* **15**, 4126 (2024).
29. Shangguan, Q., Graham, S., Sundaramoorthy, R. & White, M. F. Structure and mechanism of the type I-G CRISPR effector. *Nucleic Acids Res.* **50**, 11214–11228 (2022).
30. Staals, R. H. J. et al. Structure and activity of the RNA-targeting Type III-B CRISPR-Cas complex of Thermus thermophilus. *Mol. Cell* **52**, 135–145 (2013).

31. van der Oost, J., Westra, E. R., Jackson, R. N. & Wiedenheft, B. Unravelling the structural and mechanistic basis of CRISPR-Cas systems. *Nat. Rev. Microbiol.* **12**, 479–492 (2014).
32. Zhao, H. et al. Crystal structure of the RNA-guided immune surveillance Cascade complex in Escherichia coli. *Nature* **515**, 147–150 (2014).
33. Sofos, N. et al. Structures of the Cmr-beta Complex Reveal the Regulation of the Immunity Mechanism of Type III-B CRISPR-Cas. *Mol. Cell* **79**, 741–757.e747 (2020).
34. Behler, J. et al. The host-encoded RNase E endonuclease as the crRNA maturation enzyme in a CRISPR-Cas subtype III-Bv system. *Nat. Microbiol.* **3**, 367–377 (2018).
35. Han, W. et al. A type III-B CRISPR-Cas effector complex mediating massive target DNA destruction. *Nucleic Acids Res.* **45**, 1983–1993 (2017).
36. Szychowska, M. et al. Type III CRISPR complexes from Thermus thermophilus. *Acta Biochim. Pol.* **63**, 377–386 (2016).
37. Lopatina, A. et al. Natural diversity of CRISPR spacers of Thermus: evidence of local spacer acquisition and global spacer exchange. *Philos. Trans. R Soc. Lond. B Biol. Sci.* **374**, 20180092 (2019).
38. Wang, J., Wei, J., Li, H. & Li, Y. High-efficiency genome editing of an extreme thermophile Thermus thermophilus using endogenous type I and type III CRISPR-Cas systems. *mLife* **1**, 412–427 (2022).
39. Karneyeva, K. et al. Interference Requirements of Type III CRISPR-Cas Systems from Thermus thermophilus. *J. Mol. Biol.* **436**, https://doi.org/10.1016/j.jmb.2024.168448 (2024).
40. Du, L., Zhu, Q. & Lin, Z. Molecular mechanism of allosteric activation of the CRISPR ribonuclease Csm6 by cyclic tetra-adenylate. *EMBO J.* **43**, 304–315 (2023).
41. Artamonova, D. et al. Spacer acquisition by type III CRISPR-Cas system during bacteriophage infection of Thermus thermophilus. *Nucleic Acids Res*. **48**, 9787–9803 (2020).
42. Juranek, S. et al. A genome-wide view of the expression and processing patterns of Thermus thermophilus HB8 CRISPR RNAs. *RNA* **18**, 783–794 (2012).
43. Niewoehner, O., Jinek, M. & Doudna, J. A. Evolution of CRISPR RNA recognition and processing by Cas6 endonucleases. *Nucleic Acids Res.* **42**, 1341–1353 (2014).
44. Ohtani, N., Tomita, M. & Itaya, M. An extreme thermophile, Thermus thermophilus, is a polyploid bacterium. *J. Bacteriol.* **192**, 5499–5505 (2010).
45. Mitkas, A. A., Valverde, M. & Chen, W. Dynamic modulation of enzyme activity by synthetic CRISPR-Cas6 endonucleases. *Nat. Chem. Biol.* **18**, 492–500 (2022).
46. Hayes, R. P. et al. Structural basis for promiscuous PAM recognition in type I-E Cascade from E. coli. *Nature* **530**, 499–503 (2016).
47. Xiao, Y. et al. Structure basis for directional R-loop formation and substrate handover mechanisms in type I CRISPR-Cas system. *Cell* **170**, 48–60 e11 (2017).
48. Lin, J. et al. DNA targeting by subtype I-D CRISPR-Cas shows type I and type III features. *Nucleic Acids Res.* **48**, 10470–10478 (2020).
49. Staals, R. H. et al. RNA targeting by the type III-A CRISPR-Cas Csm complex of Thermus thermophilus. *Mol. Cell* **56**, 518–530 (2014).
50. Li, Y. & Bondy-Denomy, J. Anti-CRISPRs go viral: the infection biology of CRISPR-Cas inhibitors. *Cell Host Microbe*. https://doi.org/10.1016/j.chom.2020.12.007 (2020).
51. Koonin, E. V. & Krupovic, M. Phages build anti-defence barriers. *Nat. Microbiol.* **5**, 8–9 (2020).
52. Katz, M. A. et al. Diverse viral cas genes antagonize CRISPR immunity. *Nature* **634**, 677–683 (2024).
53. Hu, C. et al. Allosteric control of type I-A CRISPR-Cas3 complexes and establishment as effective nucleic acid detection and human genome editing tools. *Mol. Cell* **82**, 2754–2768.e2755 (2022).
54. Zaayman, M. & Wheatley, R. M. Fitness costs of CRISPR-Cas systems in bacteria. *Microbiology* **168**, https://doi.org/10.1099/mic.0.001209 (2022).
55. Vale, P. F. et al. Costs of CRISPR-Cas-mediated resistance in Streptococcus thermophilus. *Proc. Biol. Sci.* **282**, 20151270 (2015).
56. Brouns, S. J. et al. Small CRISPR RNAs guide antiviral defense in prokaryotes. *Science* **321**, 960–964 (2008).
57. Workman, R. E. et al. Anti-CRISPR proteins trigger a burst of CRISPR-Cas9 expression that enhances phage defense. *Cell Rep.* **43**, 113849 (2024).
58. Medina-Aparicio, L. et al. The CRISPR/Cas immune system is an operon regulated by LeuO, H-NS, and leucine-responsive regulatory protein in Salmonella enterica serovar Typhi. *J. Bacteriol.* **193**, 2396–2407 (2011).
59. Westra, E. R. et al. H-NS-mediated repression of CRISPR-based immunity in Escherichia coli K12 can be relieved by the transcription activator LeuO. *Mol. Microbiol.* **77**, 1380–1393 (2010).
60. Patterson, A. G., Chang, J. T., Taylor, C. & Fineran, P. C. Regulation of the Type I-F CRISPR-Cas system by CRP-cAMP and GalM controls spacer acquisition and interference. *Nucleic Acids Res.* **43**, 6038–6048 (2015).
61. Koyama, Y., Hoshino, T., Tomizuka, N. & Furukawa, K. Genetic transformation of the extreme thermophile Thermus thermophilus and of other Thermus spp. *J. Bacteriol.* **166**, 338–340 (1986).
62. Li, H., Angelov, A., Pham, V. T., Leis, B. & Liebl, W. Characterization of chromosomal and megaplasmid partitioning loci in Thermus thermophilus HB27. *BMC Genom.* **16**, 317 (2015).
63. Bolger, A. M., Lohse, M. & Usadel, B. Trimmomatic: a flexible trimmer for Illumina sequence data. *Bioinformatics* **30**, 2114–2120 (2014).
64. Langmead, B. & Salzberg, S. L. Fast gapped-read alignment with Bowtie 2. *Nat. Methods* **9**, 357–359 (2012).
65. Wang, L., Wang, S. & Li, W. RSeQC: quality control of RNA-seq experiments. *Bioinformatics* **28**, 2184–2185 (2012).
66. Liao, Y., Smyth, G. K. & Shi, W. featureCounts: an efficient general purpose program for assigning sequence reads to genomic features. *Bioinformatics* **30**, 923–930 (2014).
67. Cock, P. J., Fields, C. J., Goto, N., Heuer, M. L. & Rice, P. M. The Sanger FASTQ file format for sequences with quality scores, and the Solexa/Illumina FASTQ variants. *Nucleic Acids Res.* **38**, 1767–1771 (2010).
68. Scheltema, R. A. et al. The Q Exactive HF, a Benchtop mass spectrometer with a pre-filter, high-performance quadrupole and an ultra-high-field Orbitrap analyzer. *Mol. Cell Proteom.* **13**, 3698–3708 (2014).
69. Prianichnikov, N. et al. MaxQuant software for ion mobility enhanced shotgun proteomics. *Mol. Cell Proteom.* **19**, 1058–1069 (2020).
70. UniProt Consortium. UniProt: the universal protein knowledgebase in 2021. *Nucleic Acids Res.* **49**, D480-d489 (2021).

Acknowledgements

We would like to thank the National Key Laboratory of Agricultural Microbiology Core Facility for technical support. This study was supported by the National Key Research and Development Program of China (2022YFA0912200), National Natural Science Foundation of China (32170096), and Fundamental Research Funds for the Central Universities (2662022SKPY001).

Author contributions

Yingjun Li and Junwei Wei conceived and supervised the project. Junwei Wei and Yingjun Li designed experiments and analyzed experimental data. Junwei Wei performed experiments. Yuan Shao, Yuqian Liang, Xuying Bu, Wen Zhou, and Yunxiang Liang assisted with the experiments, data analysis, and discussions. Yingjun Li and Junwei Wei wrote the manuscript. All authors contributed to and approved the final version.

Competing interests
The authors declare no competing interests.

Additional information
Supplementary information The online version contains supplementary material available at https://doi.org/10.1038/s42003-025-08223-4.

Correspondence and requests for materials should be addressed to Yingjun Li.

Peer review information *Communications Biology* thanks Rui Wang and the other, anonymous, reviewers for their contribution to the peer review of this work. Primary Handling Editor: Mengtan Xing.